Proceedings World Geothermal Congress 2010
Bali, Indonesia, 25-29 April 2010

Case Study: Development of a Numerical Model by a Multi-Disciplinary Approach, Rotokawa Geothermal Field, New Zealand

Deborah Bowyer[1] and Richard Holt[2]

[1]Mighty River Power, Hamilton, New Zealand; [2]Geothermal Science Inc, Irvine, California, USA

[1]deborah.bowyer@mightyriver.co.nz; [2]rholt@geothermalscience.com

Keywords: Rotokawa, numerical model, modelling, geology, geophysics, reservoir engineering, TETRAD, reservoir simulation

ABSTRACT

A comprehensive multi-disciplinary conceptual model was developed for the Rotokawa Geothermal Field by integrating natural state temperatures, geology, geophysics, geochemistry, tracer test results and downhole pressures into a complete geoscientific description of the resource. Through a numerical model construction process, each component of the conceptual model was converted into numerical model simulation code for the reservoir simulator TETRAD. This resulted in a realistic initial version of the numerical model. The numerical model was further developed by implementing a deterministic, forward modelling approach while still maintaining adherence to all aspects of the conceptual model. The result was a numerical model that retained the features of the conceptual model and accurately reproduced measured data. The numerical simulation has both demonstrated the consistency of the conceptual model and provided a quantitative predictive tool.

1. INTRODUCTION

The Rotokawa Geothermal Field is situated in the Taupo Volcanic Zone, about 10km east of the Wairakei Geothermal Field and 12km northeast of Taupo (Figure 1). Government agencies drilled seven investigation wells to assess the resource between 1965 and 1986 (RK1-6, RK8).

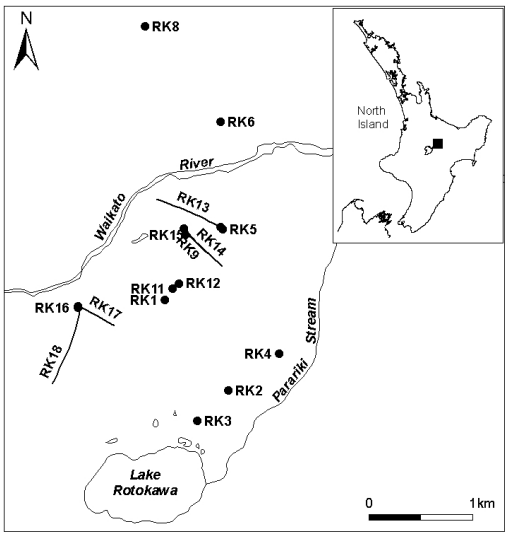

Figure 1: Location of wells in the Rotokawa geothermal Field. Insert shows location of Rotokawa in the central North Island, New Zealand.

Geothermal generation of 24MWe began in 1997. Mighty River Power acquired interest in the field through the Rotokawa Joint Venture, a joint venture with the Tauhara North No. 2 Trust, a Maori trust, in 2000. Generation was subsequently expanded to 34MWe. Between 1997 and 2005 nine further wells were drilled (RK9, RK11-18) (Figure 1). Production wells are RK5, RK9, RK13 and RK14. From 1997 to 2005 injection was into shallow wells RK1, RK11 and RK12. From 2005 injection was into deep wells RK16 and RK18. In 2007, in support of a resource consent application to expand generation from the field via construction of the 132MWe Nga Awa Purua Power Station, new conceptual and numerical models were developed. This paper discusses the process of constructing the conceptual model and converting it into a numerical model that accurately reproduces measured data, and which can be used to predict reservoir response to future development of the field.

2. CONCEPTUAL MODEL DEVELOPMENT

A conceptual model for the Rotokawa Geothermal Field was developed along five cross-section lines (Figure 2) chosen to maximise the number of wells per line, and hence data that could be utilised, and to cover the northwestern edge of the field where wells have not been drilled. The two lines that include the greatest number of wells, and hence require the least amount of extrapolation (lines A-A' and D-D'), are shown in Figures 3 and 4, respectively. Primary inputs to the conceptual model development process are geology and natural state temperatures. Geophysics, geochemistry, tracer test results and downhole pressures provide supporting information.

2.1 Geology

The subsurface geology of the Rotokawa Geothermal Field has been interpreted from drill cuttings and cores (Figures 3 & 4). Basement Greywacke is overlain by the Rotokawa Andesite, a sequence of andesite lava flows and breccias up to 2000m thick. Differences in the elevation at which the Basement Greywacke and Rotokawa Andesite are encountered in wells suggest the occurrence of a series of SW-NE striking normal faults, parallel to the structural trend of the Taupo Volcanic Zone, which have resulted in a structural trough (graben) between RK4 and RK6. RK17 is the only well that can be confirmed as having intersected one of these faults (Figures 2 & 4).

Overlying the Rotokawa Andesite, and infilling the graben, are the volcaniclastic and sedimentary deposits of the Tahorakuri and Waikora formations (members of the Reporoa Group), which are in turn overlain by the Wairakei Ignimbrite. The elevation of the top of this ignimbrite is relatively constant across the field suggesting no, or very little, reactivation of the graben-forming faults since its deposition. Lack of Wairakei Ignimbrite in RK16-RK18 suggests that the ignimbrite ponded against a fault scarp to

the east of these wells. Overlying Wairakei Ignimbrite are the rhyolitic tuffs, ashes and breccias of the Waiora Formation. Haparangi Rhyolite lavas and breccias occur within the Waiora Formation, which is then overlain by mudstones, siltstones and sandstones of the Huka Formation intercalated with the Parariki hydrothermal eruption breccias.

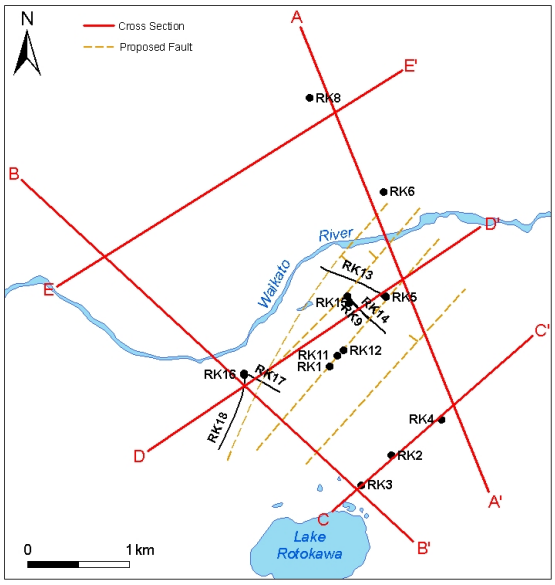

Figure 2: Orientation of cross section lines used in development of the conceptual model. Proposed faults (in their approximate position at the top of the Rotokawa Andesite) are also shown.

The surface geology at Rotokawa is dominated by rhyolite domes in the north (around RK8) and elsewhere by pumice alluvium, tuff breccia and hydrothermal eruption breccias.

Permeable zones in the deep wells (RK5, RK9, RK13-14, RK16-17) indicate that the geothermal reservoir is primarily within the Rotokawa Andesite. In RK17 permeable zones occur on either side of the fault intersection, suggesting that reservoir permeability is controlled, at least in part, by fault structures. However, as other wells are not known to directly intersect fault structures, other factors (e.g. lava flow boundaries, cooling joints) must also play a role in providing permeability and controlling fluid flow. Permeable zones in the shallow wells (RK1, RK11-12), and fluid losses while drilling, indicate the occurrence of high permeability in the Waiora Formation and Haparangi Rhyolite.

A propylitic alteration mineral assemblage (including mordenite, wairakite, epidote, clinozoisite, quartz, illite, chlorite, adularia, albite and calcite) occurs within the geothermal reservoir, indicating deposition from near neutral pH, chloride waters. At shallower levels, in the Waiora Formation and Haparangi Rhyolite, the occurrence of goethite, kaolinite, alunite and dickite is indicative of the presence of potentially corrosive CO_2-rich/bicarbonate and sulphate fluids (Bowyer et al., 2008).

From the five cross sections, maps were created showing the geology at specific elevations, a selection of which are shown in Figure 5. The influence of proposed faults on the distribution of geological formations is evident at 1000m, 1500m and 2000m below sea level, while at shallower levels the geology is controlled by the distribution of rhyolite lava domes and flows.

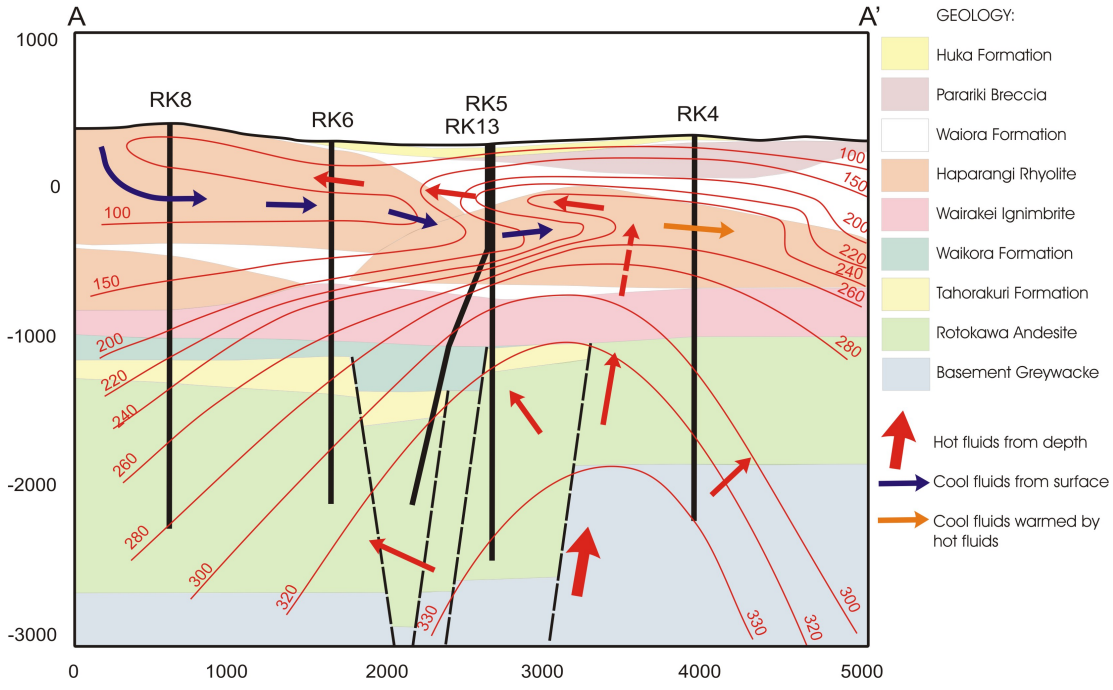

Figure 3: Cross section A-A' of the Rotokawa conceptual model (approximately north-south) showing well tracks, geology, proposed faults and natural state temperature isotherms (in degrees C and meters bsl).

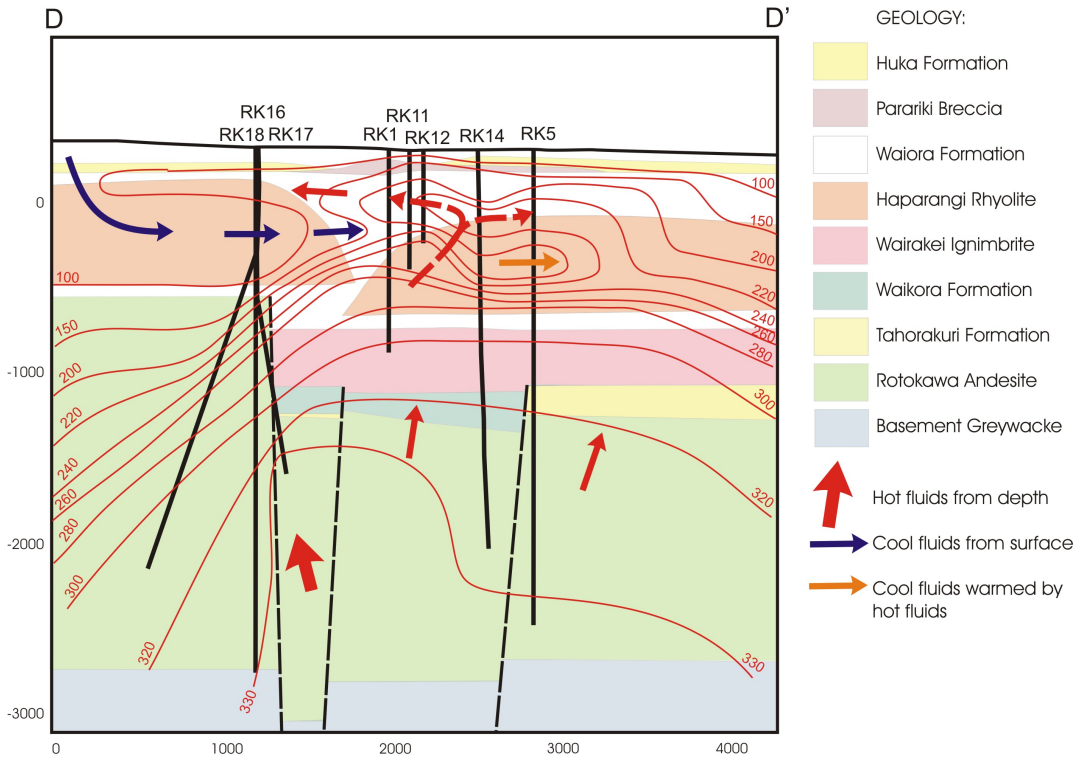

Figure 4: Cross section D-D' of the Rotokawa conceptual model (approximately east-west) showing well tracks, geology, proposed faults and natural state temperature isotherms (in degrees C and meters bsl).

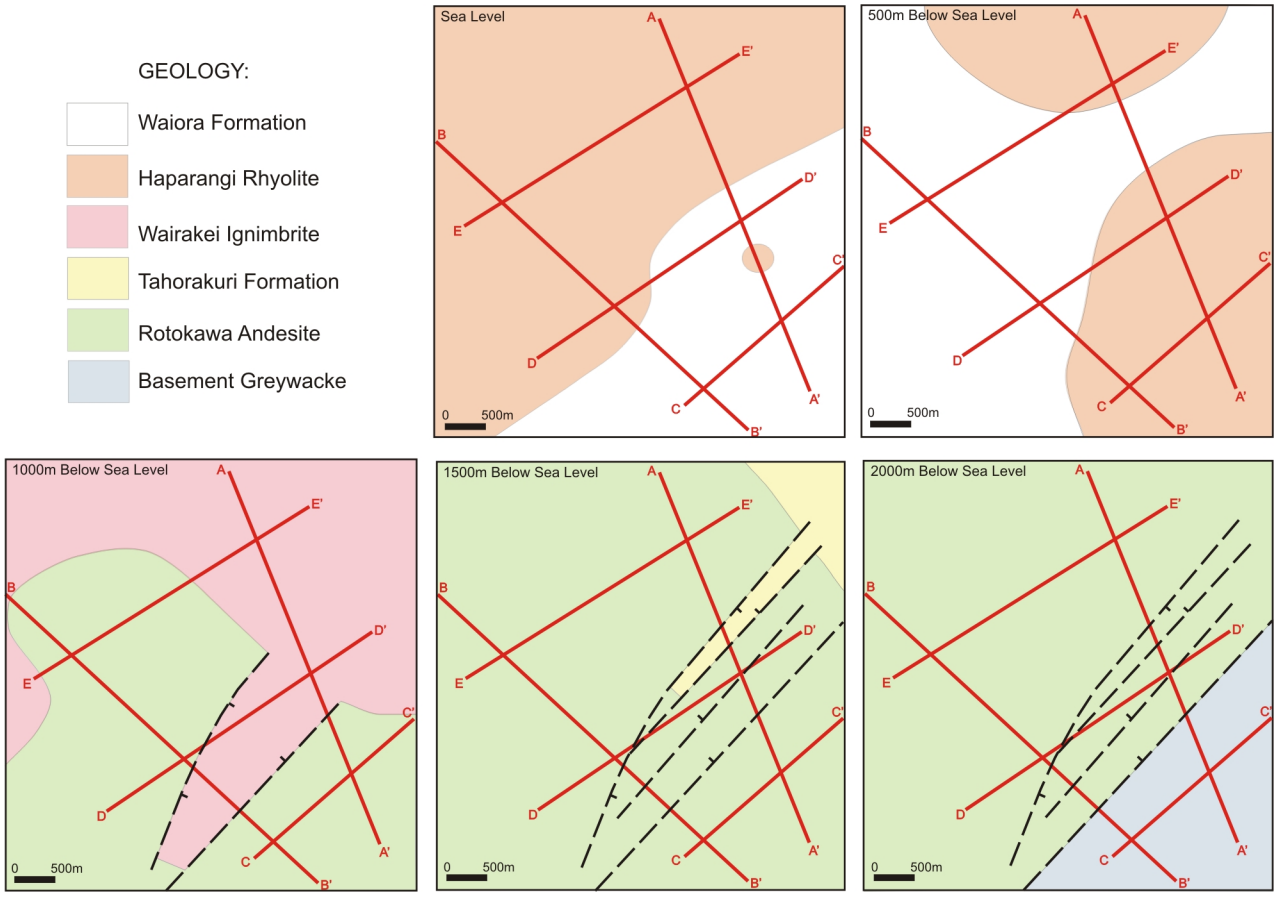

Figure 5: Geological maps at sea level and 500m, 1000m, 1500m and 2000m below sea level.

2.2 Natural State Temperatures

Natural state temperature isotherms have been interpolated from stable downhole temperatures (Figures 3 & 4). The hottest wells in the field are RK4, RK5 and RK17 with bottom hole temperatures of at least 330°C, suggesting that the deep upflow for the geothermal system lies between these wells. Bottom hole temperatures decline to the north with ~310°C in RK6 and ~280°C in RK8. RK17 encountered the shallowest occurrence of 330°C fluid at approximately 1500m below sea level. In the west the fault intersected by RK17 influences the shape of the deep isotherms, suggesting that it is a major conduit for upflow and that it defines the western boundary of the geothermal reservoir. With the exception of RK4, all wells show a temperature reversal above approximately 700m below sea level.

Maps were created showing the distribution of natural state isotherms at specific elevations, a selection of which are shown in Figure 6. The map at 2000m below sea level shows the deep upflow for the geothermal system between RK4, RK14 and RK17. The upflow associated with the fault encountered in RK17 can be identified as a small area of fluid of >330°C at 1500m below sea level. At 500m below sea level an upflow of >280°C fluid from the geothermal reservoir into shallower aquifers can be seen between RK1, RK3 and RK4.

2.3 Supporting Information

In conjunction with drilling results, MT-TDEM was used to derive a probable boundary for the geothermal resource. This boundary was then used to guide the shape of isotherms at the edges of the field, particularly in the northwest where no well data is available.

High chloride content in fluid discharged from RK4, with progressive dilution in wells to the north, is consistent with the location of the deep upflow between RK4, 14 and 17, as suggested by natural state temperatures.

A tracer test in 1998 showed no returns from shallow injection wells (RK1, RK11-12) to adjacent deep production wells (RK5 & 9), suggesting the lack of a rapid or preferred flow path between the shallow injection aquifer (Haparangi Rhyolite and Waiora Formation) and geothermal reservoir (Rotokawa Andesite). A lack of connection was also suggested by changes in downhole pressure during the first

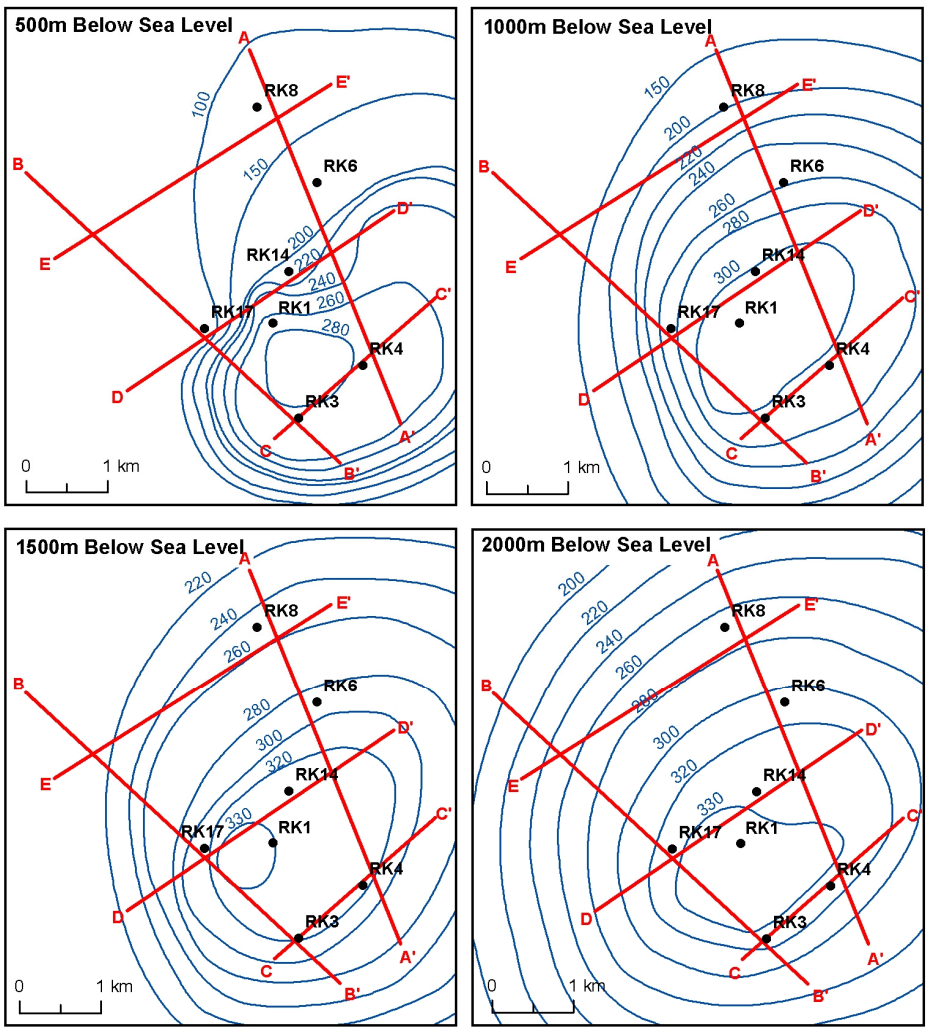

Figure 6: Natural state temperature isotherms (°C) at 500m, 1000m, 1500m and 2000m below sea level (selected wells are also shown).

eight years of development. Pressures in the shallow injection aquifer increased over this period, while pressures in the deeper geothermal reservoir declined. No tracer was seen to migrate from the shallow injection zone to the deeper geothermal reservoir, even though it was over-pressured compared to the deeper geothermal reservoir. Pressure interference testing also showed lack of connection between the shallow injection zone and the deeper production reservoir. The Wairakei Ignimbrite, which is continuous over most of the field, is considered to provide a reasonably continuous permeability barrier between the shallow injection aquifer and geothermal reservoir. Shallow pressures were seen to be high at the base of the clay-rich Huka Formation, suggesting that this formation is capping the shallow injection aquifer.

A tracer test in 2006 identified a SW-NE oriented preferred flow direction in the geothermal reservoir from RK18 to RK17 and RK13. This is consistent with the proposed SW-NE orientation of normal faults as suggested by differing elevations for the top of the Basement Greywacke and Rotokawa Andesite in wells.

2.4 The Rotokawa Conceptual Model

High temperature (>330°C) fluid upflows from depth in the area between RK4, RK14 and RK17 (Figures 3 & 4). Faults are major conduits for fluid flow in the Rotokawa Andesite, allowing upflow of >330°C fluid to 1500m below sea level to the east of RK17. Fluids in the andesite-hosted geothermal reservoir follow a preferred SW-NE flow direction, and outflow to the north and northeast.

Cool inflows from the surface extend across the area at depths up to 500m below sea level, flowing primarily through Haparangi Rhyolite lavas and breccias and potentially preferentially favouring boundaries between lava flows. These cool inflows remain separate from the deeper geothermal reservoir due to the occurrence of the largely impermeable Wairakei Ignimbrite which acts as a cap to the reservoir.

However, hot (>280°C) fluids from the deep reservoir are "leaking" upwards through the Wairakei Ignimbrite in the area between RK1, 3 and 4. Why a leak occurs at this location is unclear, although it may be related to hot fluid upflow from depth along underlying faults. From the zone of leakage these hot fluids flow laterally, primarily through the upper parts of the Haparangi Rhyolite and overlying Waiora Formation, overlying the cooler inflows from the surface and accounting for the shallow temperature reversals seen in most wells.

2.5 Preparation for Conversion to a Numerical Model

Conversion of the conceptual model to a numerical model involved digitisation of the geological and natural state temperature maps to derive a series of x,y,z coordinates for formation boundaries and isotherms. As the maps covered a smaller area than the numerical model, formation boundaries and isotherms were extrapolated to the numerical model boundaries prior to digitisation. Coordinates were also derived for the proposed reservoir faults and the geophysically-defined probable resource boundary.

3. NUMERICAL MODEL DEVELOPMENT

Over the past two decades, numerical reservoir simulation has become a predominant method by which geothermal reservoirs are analyzed and predictions are made about their future state and performance (O'Sullivan 2000). In addition to making predictive forecasts, geothermal reservoir simulation is equally useful as a method to quantitatively test a conceptual model of a geothermal reservoir. If a numerical model is consistent with a conceptual model, while accurately matching measured data, then this adds to the confidence in the validity of the conceptual model. Numerical modelling was implemented at Rotokawa to both provide a tool for making predictive forecasts and to quantitatively test the validity of the conceptual model.

The reservoir simulation software TETRAD was used for the numerical modelling. TETRAD is a three-dimensional, single or dual porosity, multi-phase, multi-component, thermal, finite-difference simulator (Vinsome and Shook, 1993). In the geothermal industry, TETRAD is widely used by operating companies, consulting firms, and research organizations. Additionally, a published research study by a U.S. based national laboratory concluded that TETRAD provides valid solutions to the complex equations in geothermal applications (Shook and Faulder, 1991). Specialized software PetraSim was used in the preparation of TETRAD input files, and in the viewing of the three-dimensional distribution of input parameters and output simulation variables. In addition, TecPlot software was used in advanced three-dimensional visualizations and animations of dynamic reservoir simulation output. All software programs used are commercially available.

3.1 Numerical Model Grid

The first step in creating a numerical model is designing an appropriate computational grid. The numerical model covers an area of 10.5 by 9 km and is centered on the Rotokawa steamfield. The model grid was rotated 44.1 deg to the NW to allow the x and y axis of the model to lie relatively parallel to SW-NE strike of the fractures as reported in the conceptual model. Figure 7 shows the computation grid shown from above.

Figure 7: Aerial photo of the Rotokawa region that is included in the numerical model. The yellow lines are the borders of computational grid blocks.

The model contains 27 layers extending from surface to 4250m below sea level. Each layer contains 4230 blocks, for a total of 114,210 gridblocks in the computational grid. Figure 8 shows a three dimensional representation of the final simulation grid used for the Rotokawa numerical model. Horizontally, the computational grid is areally large

enough to cover the entire Rotokawa geothermal resource, extending beyond the inferred resource boundary in all directions. Vertically, the computational grid is thick enough to extend from ground surface to the origins of hot upwelling fluids below the geothermal reservoir.

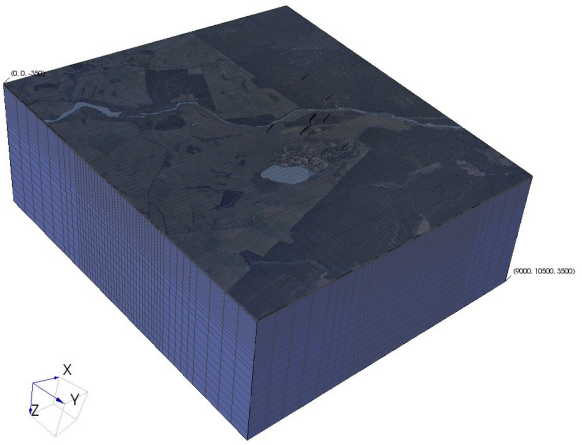

Figure 8: Three dimensional view of the computational grid.

3.2 Conversion of Conceptual Model to Numerical Model

The next step in creating the Rotokawa numerical model was to convert the conceptual model as described above, into the digital format required by the reservoir simulator TETRAD. This digitised form of the conceptual model was then translated onto the computational grid as three dimensional distributions of rock properties and boundary conditions.

Stratigraphy was modeled by digitizing the geologic contour maps showing the distribution of rock type (as shown in Figure 5). This was done for each of the 17 of the 27 layers in the model, with the remaining 10 layers assigned properties based on their nearest neighboring layer. This resulted in a three-dimensional distribution of rock type throughout the numerical model. This process explicitly accounts for the structure in the model. A sample of the digitized rock type maps and their assignment in the numerical model is shown in Figure 9. The rock type assignment process was configured such that rock type assignments for blocks that were within the inferred reservoir boundary were assigned a rock-type code for being within the reservoir volume. The same rock types within the inferred reservoir volume were assigned higher permeability than the same rock type outside.

Faulting was accounted for by placing several discrete faults that extend through the andesite and through the greywacke to a deep source area. These faults have enhanced vertical permeability and enhanced lateral permeability in the direction from SW to NE (which is aligned with model direction X). In this deep source area, hot fluid is flowed into the model as a mass flux. The hot fluid migrates up through these faults. At depth, the faults extend into greywacke, and the greywacke is modeled everywhere as low permeability except in the location of these faults.

The hot upwelling fluid then continues to flow upward and into the andesite formation which is the primary deep reservoir rock at Rotokawa. A dual porosity formulation was used across the entire model to enhance the modelling of the flow processes occurring in the reservoir. In the conceptual model, the andesite is identified as a rock unit that has some primary (matrix) permeability, in addition to the enhanced secondary (fracture) permeability around faults. This was modeled by assigning moderate fracture permeability to the andesite rocks that were inside the inferred reservoir boundary. Rocks outside the inferred reservoir volume were assigned low fracture permeability.

In the model, rock units were modeled as having bulk matrix porosities in the range of 5 to 20%. The volume-weighted average in the numerical model is approximately 10%. Both the range and average are consistent with measured values of porosity that were available. Fracture porosity was set to 1% throughout the entire model. Fracture permeability ranged from 240 millidarcies down to 0.09 millidarcies. Matrix permeability ranged from 120 millidarcies down to 0.01 millidarcies.

3.3 Boundary Conditions on the Numerical Model

The top of the model is a constant pressure boundary that represents atmospheric pressure and is set at a constant temperature of 20 ^{o}C and pressure of 1 bara. This boundary on top of the model is configured such that fluid can discharge to the surface but only gas can flow back down into the model. The exception is a constant influx of cold water that represents infiltration of 5% of average local precipitation.

The sides of the model are closed boundaries with respect to heat and mass, with the exception of constant pressure sinks on the NW and SE edges of the model to represent subsurface discharge out of the system. This was necessary to match the strong shallow temperature reversals in the system (see Figures 3 and 4).

The source upflow area is set to be the area within the 320 ^{o}C degree contour on the 2000m below sea level isotherm map. On the bottom of the model (at 4250m below sea level) 105 kgs of water at 1600 KJ/kg is flowed into the model under constant mass flux conditions. This water contains dissolved carbon dioxide and chloride in the following amounts: Dissolved carbon dioxide 0.8% by mass and chloride 1500 ppm by mass. These dissolved components upflow within the source fluid and mix with cross-flowing and descending fresher waters. The result is a close match to the measured values of these components in the production wellfield.

3.4 Simulation of the Natural State Conditions

With the model constructed as described above, the natural state conditions were simulated. The process of achieving a match involved a process of manual iteration. The rock properties and boundary flows were first set. The temperatures and pressures were then set to background hydrostatic conditions. Then the model was run for 1,000,000 years of simulated time to create a steady-state thermally anomaly.

In an iterative process, the simulated natural state results were compared to measured data, primarily distributions of pressure, temperature, and chemistry. Upon evaluation of the results of each iteration, adjustments were made to the assignment of permeability for each type of rock. A new model version was created and again run for 1,000,000 years of simulated time. In creating the new model version after each iteration, judgment and trial-and-error were used in conjunction to determine adjustments to make to improve the match. In all iterations, the range of parameters used, distribution of rock types, and configuration of boundary

conditions was held to be consistent with the conceptual model.

The entire simulation matching process was done deterministically without the use of automatic history matching or inverse modelling technique. The initial version of the model was obtained relatively quickly. This is believed to be a result of having the numerical model closely follow the conceptual model. Figure 10 shows a three dimensional view of the final simulated natural state temperatures as a set of temperature isosurfaces. This figure clearly shows a simulated hot upflow of geothermal fluids flowing first vertically, and then laterally into shallow aquifers creating strong temperature reversals. This is fully consistent with the conceptual model.

Figures 11 and 12 show two vertical slices through the model and show simulated natural state temperatures. Figure 11 shows simulated natural state temperatures on geologic cross section line A-A' (see Figure 3), and Figure 12 shows simulated natural state temperatures on geologic cross section line D-D' (see Figure 4). Figures 3 and 4 show the interpreted temperatures from the conceptual model on the same cross sections. A comparison of Figure 3 and 4 to Figures 11 and 12 gives a direct comparison between simulated and measured/interpreted temperatures. A high quality match is obtained in both cases.

4. CONCLUSIONS

- The numerical model closely adheres to all aspects of the conceptual model and the numerical model closely matches measured data. In developing the numerical model, only deterministic techniques were used, as opposed to automatic history matching or inverse modelling.
- A comprehensive multi-disciplinary conceptual model was developed for the Rotokawa Geothermal Field. This confidence in the conceptual model's validity is increased because it has successfully formed the basis of a numerical model that closely matches measured data.
- The numerical model's basis is a realistic and accurate conceptual model and the numerical model accurately represents measured data. Therefore, there is confidence in using the numerical model as a reliable predictive tool.

REFERENCES

Bowyer, D., Bignall, G., and Hunt, T.: Formation and Neutralisation of Corrosive Fluids in the Shallow Injection Aquifer, Rotokawa Geothermal Field, New Zealand, *Geothermal Resources Council Transactions*, **32**, (2008), 201-205.

O'Sullivan, M. J., Pruess, K. & Lippmann M. J. 2000. Geothermal Reservoir Simulation: The State-Of-Practice and Emerging Trends, Proceedings World Geothermal Congress 2000, Kyushu – Tohoku, Japan, May 2000.

Shook, M. & Faulder, D. 1991. Validation of a Geothermal Simulator, EG & G Report #EP-9851, October 1991

Vinsome, K.W & Shook M.1993, Multi-Purpose Simulation, Journal of Petroleum Science and Engineering, vol 9, pages 29-38, 1993

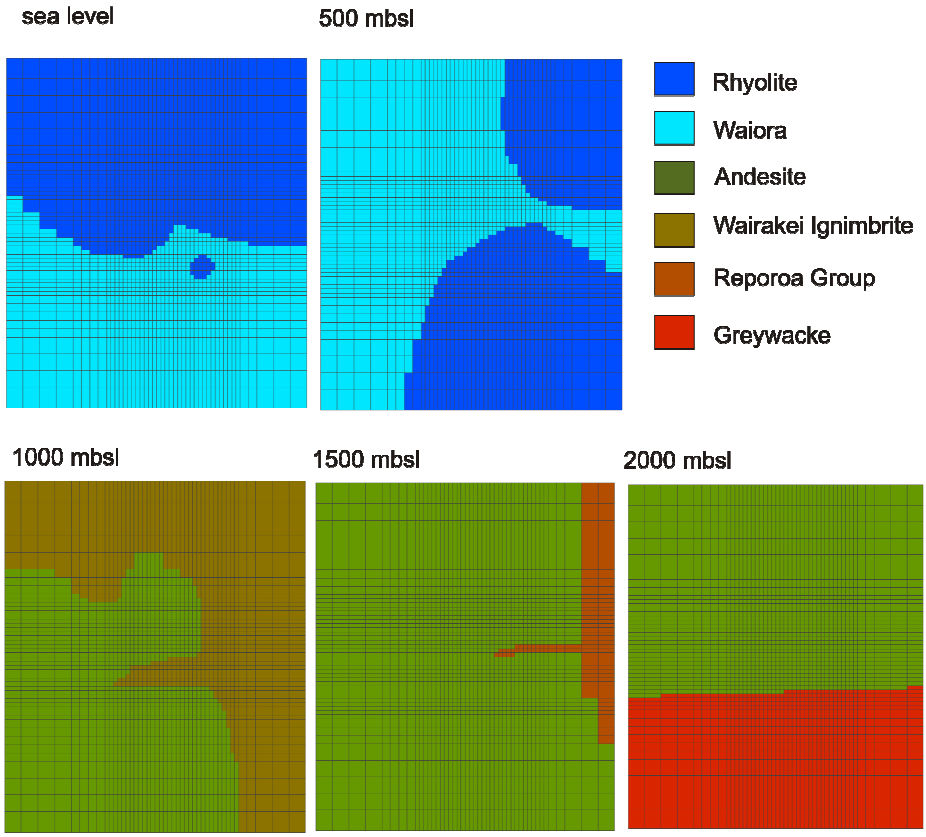

Figure 9: Simulated rock type maps at sea level and 500m, 1000m, 1500m and 2000m below sea level.

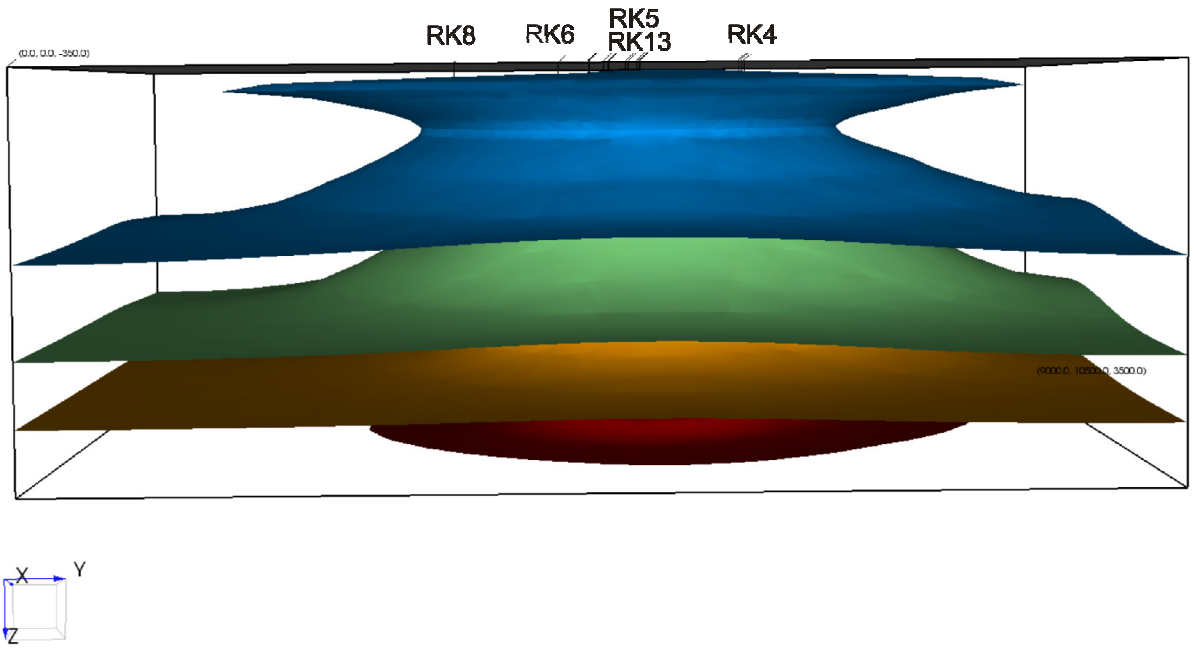

Figure 10: Simulated natural state temperature isosurfaces for temperatures of 100, 175, 250, and 330 degrees C.

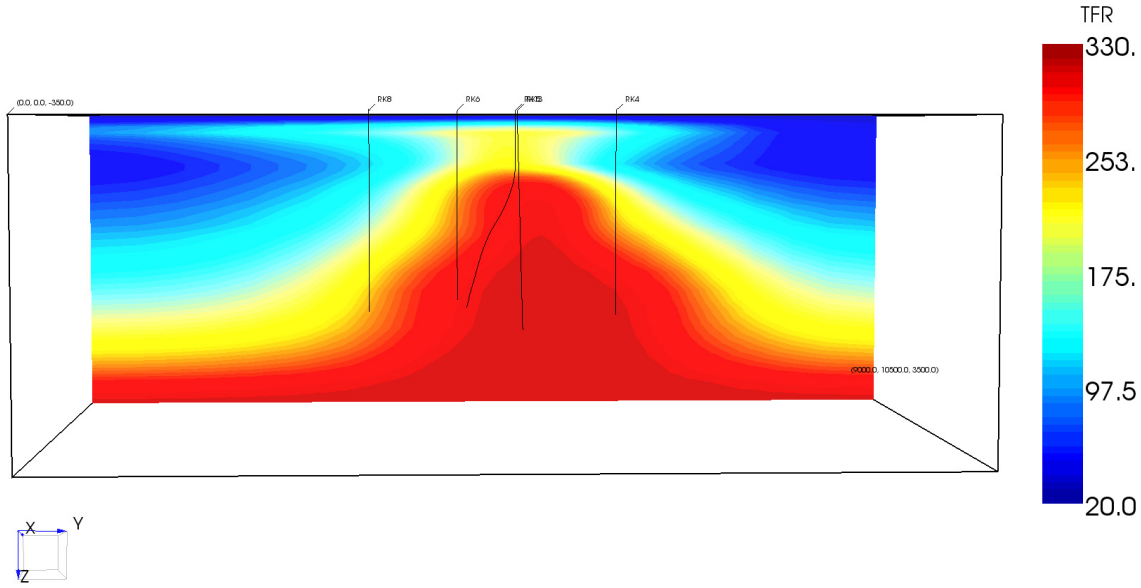

Figure 11: Simulated natural state temperatures on geologic cross section A-A', compare to Figure 3, temperatures are in degrees C.

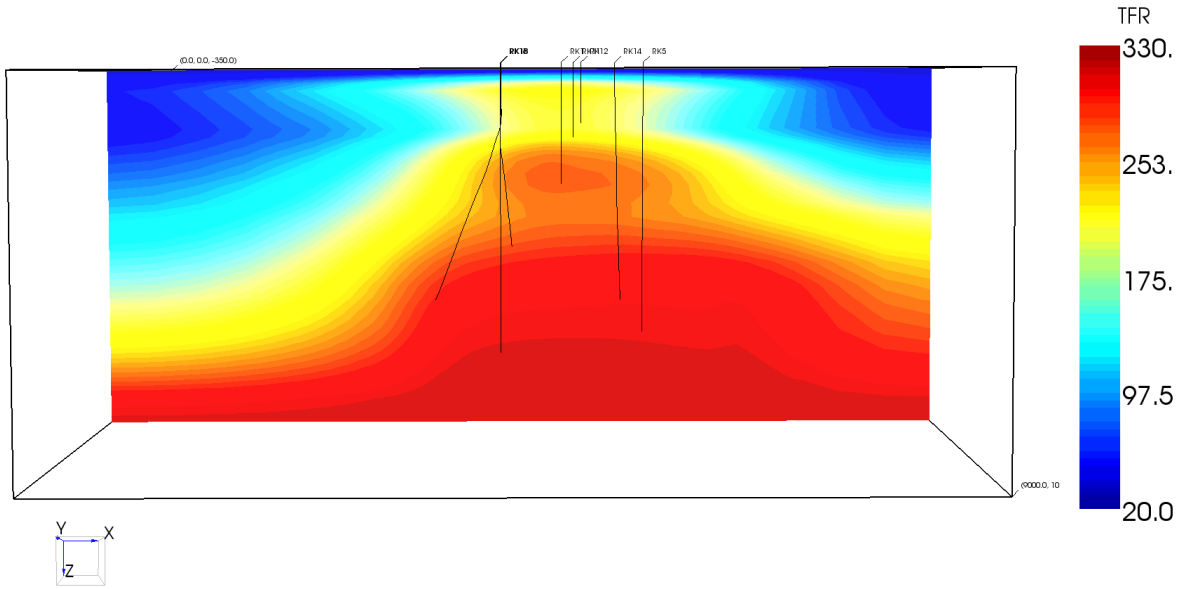

Figure 12: Simulated natural state temperatures on geologic cross section D-D', compare to Figure 4, temperatures are in degrees C.